LUNAR POLARIMETRIC IMAGING AT SMALL PHASE ANGLES. N. Opanasenko[1], Y. Shkuratov[1], G. Videen[2], V. Kaydash[1], V. Korokhin[1], Ye. Surkov[1], S. Velichko[1], D. Stankevich[1], Yu. Velikodsky[3], Sungsoo S. Kim[4], Young-Jun Choi[5], Chae Kyung Sim[5], Minsup Jeong[5], [1]Institute of Astronomy, V. N. Karazin National University, 35 Sumska St, Kharkiv, 61022, Ukraine, [2]Space Science Institute, 4750 Walnut St. Suite 205, Boulder CO 80301, USA, [3]National Aviation University, Lubomyr Husar Ave. 1, Kyiv 03058, Ukraine, [4]Humanitas College, Global Campus, Kyung Hee University, Gyeonggi 17104, Korea, [5]Korea Astronomy and Space Science Institute, Daejeon 34055, Korea.

Introduction: At small phase angles α, the Moon reveals a negative polarization branch in the sense of the definition, $P(\alpha) = (I_\perp - I_\parallel)/(I_\perp + I_\parallel)$, where $I_\perp$ and $I_\parallel$ are intensity components [e.g., 1,2]. At $\alpha < 50^\circ$ the function $P(\alpha)$ has a shape near to parabolic. The function can be characterized with parameters $P_{\min}$, α_{inv}, and h that are the depth of the branch, inversion angle (where $P = 0$), and slope of $P(\alpha)$ at $\alpha = \alpha_{\text{inv}}$, respectively. For the Moon $|P_{\min}| \approx 1\%$ and $\alpha_{\text{inv}} \approx 23^\circ$. These three parameters have only barely been studied over a few selected areas with Earth-based observations [2-5]. These parameters have yet fairly poor interpretation, and they are independent of other optical characteristics. They potentially are important in future explorations of the Moon and other atmosphereless celestial bodies with spacecraft.

The Korea Pathfinder Lunar Orbiter (KPLO), scheduled for launch in 2022 as the first step of the Korean Lunar Exploration Program, will orbit the Moon at an altitude of 100 ± 30 km during its nominal mission of up to 12 months. The spacecraft will map the polarization characteristics of the Moon using the Wide-Angle Polarimetric Camera (*PolCam*). In particular, these measurements can be used to map the parameters α_{inv}, $|P_{\min}|$, and h [6,7].

Observations, processing, and results: In anticipation of KPLO data, we map the polarimetric parameters using data of photometric and polarimetric observations of the Moon, which were conducted at the Maidanak Observatory (Uzbekistan) using the 60-cm Zeiss-600 telescope [4,8]. For the lunar observations we used a CMOS camera with an array 5184x3456 pixels with light filters R(0.61 μm), G(0.52 μm), and B(0.48 μm). Data obtained at 0.52 μm here are used. The camera is equipped with a polarizer. A series of observations of an area consists of 12 full rotations of the polarizer. In each rotation, 8 positions of the polarization axis are used for measurements. We study here a west portion of the lunar nearside, which comprise Mare Nubium (Fig. 1a), using 20 series of measurements at the following phase angles: -39.75º, -38.12º, -36.42 º, -29.24º, -26.67º, -17.65º, 8.41º, 9.69º, 10.23º, 10.66º, 22.3º, 23.28º, 23.94º, 24.61º, 28.14º, 28.23º, 31.54º, 38.89º, 39.57º, 46.78º with resolution near 0.7".

The primary image processing includes accounting for dark current and separation of flat field. The latter was calculated using observations of the evening or morning sky. Instrumental polarization parameters have been assessed also using the star-polarimetric standards and measuring the Arago point, the point of the sky near sunset or sunrise, where the degree of polarization is close to zero. We also made a Gaussian convolution of images in order to decrease the noise contribution, then, images were coregistered with the rubber-sheet algorithm [9] and averaged for each position of polarizer axis. Next, the relative intensity I and polarization degree P, were calculated.

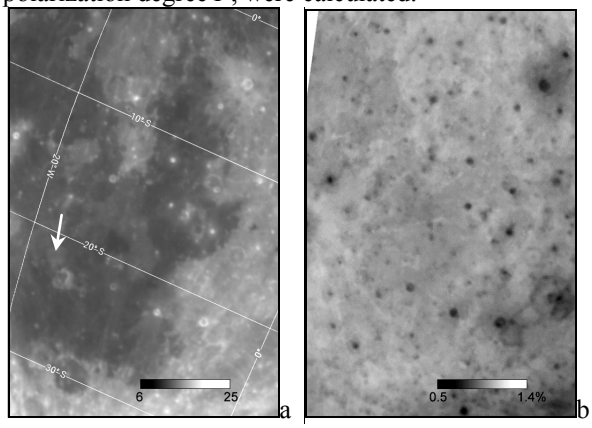

a b

Figure 1. (a) Map of the equigonal albedo at $\alpha = 9.5^\circ$; (b) Map of the parameter $|P_{\min}|$ calculated with polarimetric measurements at the six phase angles.

A photometric calibration was carried out using the Akimov disk function as discussed in [2]. We used the least-square method and carried out an approximation of the phase dependences of polarization degree in each image pixel with a polynomial of third degree with zero at $\alpha = 0$:

$$P(\alpha) = C_1\alpha^3 + C_2\alpha^2 + C_3\alpha, \quad (1)$$

where C_1, C_2, and C_3 are constants for each pixel. Equation (1) allows computation of the polarimetric parameters $|P_{\min}|$, α_{inv}, and h, accounting for non-parabolic shape of $P(\alpha)$.

The map of $|P_{min}|$ is shown in Fig. 1b. We note that bright craters have low values of $|P_{min}|$. This confirms results presented in [3]. The highest $|P_{min}|$ is characteristic of rather dark, but not darkest, areas. Figure 2a,b show images of the parameters α_{inv} and h calculated using measurements at 20 phase angles. One may see that brighter regions have larger α_{inv}, excepting bright, young craters. Some of them even show α_{inv} smaller than that of old highland areas.

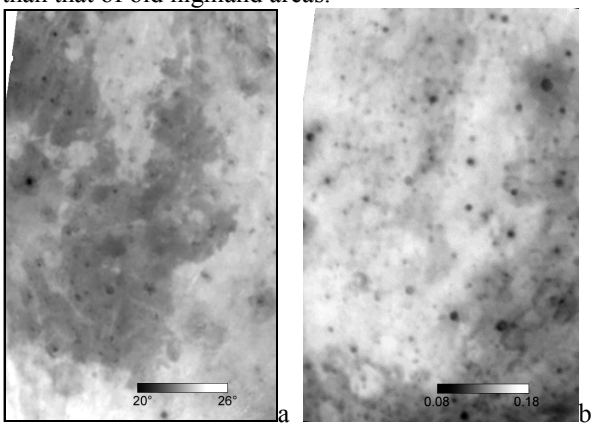

Figure 2. Maps of the parameters α_{inv} and h, respectively, (a) and (b) calculated with polarimetric measurements at the 20 phase angles.

The image of the parameter h resembles a negative of the equigonal albedo (cf. Figs. 1a and 2b). This is a consequence of the Umov effect [2].

The function $P(\alpha)$ is almost parabolic, but not exactly. That is, the equation $\alpha_{inv} = 2\alpha_{min}$ is valid only approximately. For the same scene we calculated a distribution of the angle ratio $\alpha_{inv}/\alpha_{min}$, characterizing the asymmetry of $P(\alpha)$, that is shown in Fig. 3. We see that the asymmetry increases with albedo. The craters again are exception.

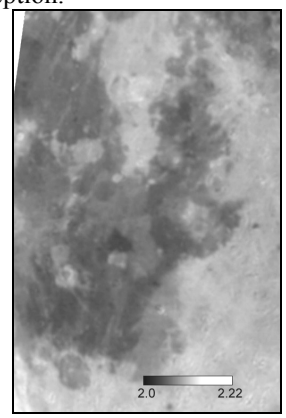

Fig. 3. Map of the angle ratio $\alpha_{inv}/\alpha_{min}$, calculated with polarimetric measurements at the 20 phase angles.

Discussion: Mare Nubium is located south of the center of the scene shown in Fig. 1a. An image of the parameter $|P_{min}|$ does not reveal a clear boundary between mare and highland regions. Several areas with intermediate albedo are more apparent using this parameter. This may indicate the increased presence of dust component of the lunar regolith.

In Fig. 1a the arrow shows a formation, which is a photometric anomaly [10]. We see that this detail is not an anomaly in the polarimetric parameters α_{inv} and h. There are a few places where the inversion angle is relative small (dark spots in Fig. 2a), which appear independent of albedo. We may suggest that these areas consist of regolith having larger concentrations of coarse particles. This feature is characteristic of immature regions. A map of the parameter h shown in Fig. 2b inversely correlates with the albedo map of Fig. 1a, as one may expect. Indeed, this correlation is the basis of using the polarimetric method of albedo determination of asteroids [11].

Conclusion: We present results of mapping the polarimetric parameters $|P_{min}|$, α_{inv}, and h for the west portion of the lunar nearside. The Mare Nubium is clearly seen in the parameters $|P_{min}|$ and α_{inv}. The photometric anomaly indicated by the arrows in Fig. 1a are not shows up in distribution of the polarimetric parameters $|P_{min}|$, α_{inv}, and h. There are several areas with relative low values of α_{inv} that may indicate coarser, and perhaps younger, regolith.

Acknowledgment: This work was supported by the NASA KPLO Participating Scientist Program NNH18ZDA001N-KPLOPSP, grant 80NSSC21K0755.

References: [1] Dollfus A., Bowell E., (1971) Astron. Astrophys., 10, 29–53. [2] Shkuratov Y., et al., (2011) Planet. Space Sci. 59. 1326-1371. [3] Opanasenko N., et al., (2020) LPSC, 51, #1156. [4] Shkuratov Y., et al., (2007) Icarus 187. 406–416. [5] Shkuratov Y., et al., (2015) In: Polarimetry of Stars and Planetary Systems / Ed. L. Kolokolova et al., Cambridge: Cambridge Univ. Press, 303–319. [6] Sim C. et al., (2019) Publ. Astron. Soc. Pacif. 131:074401. [7] Sim C.K., et al., (2020). Pub. Astron. Soc. Pacific, 132:015004 (11pp). [8] Shkuratov Y., et al., 2008. Icarus 198, 1–6. [9] Kaydash V., et al., (2012) JQSRT 113(18), 2601–2607. [10] Korokhin V., et al., (2016) Planet. Space Sci. 122, 70-87. [11] Zellner B., et al., (1977) Proc. Lunar Sci. Conf. 8-th. LPI Houston 1091–1110.